Computationaly Efficient Wideband Worst Case Model of Plane Electromagnetic Wave Diffraction by Conductive System Hull

Dzmitry Tsyanenka
EMC R&D Laboratory
Belarusian State University
of Informatics and Radioelectronics
Minsk, Belarus
emc@bsuir.by

Ivan Shakinka
EMC R&D Laboratory
Belarusian State University
of Informatics and Radioelectronics
Minsk, Belarus
emc@bsuir.by

Yauheni Arlou
EMC R&D Laboratory
Belarusian State University
of Informatics and Radioelectronics
Minsk, Belarus
emc@bsuir.by

Vladimir Mordachev
EMC R&D Laboratory
Belarusian State University
of Informatics and Radioelectronics
Minsk, Belarus
emc@bsuir.by

Eugene Sinkevich
EMC R&D Laboratory
Belarusian State University
of Informatics and Radioelectronics
Minsk, Belarus
emc@bsuir.by

Wen-Qing Guo
China Electronics Technology
Cyber Security Co., Ltd.
Chengdu, Taiyuan, China
gigigigogogo@126.com

***Abstract*—A wideband worst case model to account for the diffraction of a plane electromagnetic (EM) wave by a system hull made of a conductive material is developed. The model can be used for estimating the amplitudes of electric and magnetic fields in places of antenna mounting on the hull of an airborne vehicle (aircraft, helicopter, etc.). The model is based on consideration of the fields radiated by electric dipole in a low-frequency range and on the Fresnel approach to analysis of the diffraction in resonance- and high-frequency ranges. The use of analytical methods provides the high computational efficiency of the model. The developed model is validated by comparison of calculation results obtained by the model with results of numerical simulation performed in framework of FDTD and MOM (the ratio of the wavelength to the obstacle dimension is varied from 100 to 0.5).**

Keywords—electromagnetic compatibility, electromagnetic fields, wave diffraction, Fresnel zones

I. Introduction

For analysis of EME impact on airborne antennas and on apertures in the hull of an airborne vehicle, it is necessary to account for the diffraction of a plane electromagnetic wave by the hull. The field-to-antenna coupling model intended for express analysis and diagnostics of EMC at the level of complex systems [2]–[5] must satisfy the following requirements: physical adequacy in a wide range of values of parameters, worst case behavior, stability of calculation results against errors in initial data, and high computational efficiency.

Electromagnetic (EM) field diffraction models based on the analytical approach proposed in [1] and developed within the framework of IEMCAP program [2], [3], which are traditionally used for express analysis of EMC, provide sufficient accuracy only if the hull of the system under consideration can be represented as a set of simple geometrical shapes (cylinder, cone, plain tetragons, etc.). A generalization of the analytical approach for taking into account the diffraction by a conductive hull of arbitrary shape, based on Uniform Theory of Diffraction (UTD) [6], is valid in a wide frequency range for antenna-to-antenna coupling but is not applicable for analysis of the plane-wave diffraction. Numerical methods of computational electromagnetics (such as FEM, FDTD, MOM, GO, UTD, PO [7]–[10], as well as hybrid methods [12], [13]) used for solving the diffraction problem in framework of EMC analysis do not satisfy the requirements given above: high-frequency solutions do not have worst case behavior due to resonances, the analysis of a large set of frequencies and directions of EM wave incidence results in unacceptable computational burden.

The objective of this work is to develop a computationally efficient worst case model of diffraction of a plane electromagnetic wave with linear polarization by a conductive hull of arbitrary shape.

II. Physical Model for Analysis of Electromagnetic Wave Diffraction by Conductive Obstacle

Let us consider the linearly polarized electromagnetic plane wave of frequency f irradiating an obstacle made of the conductive material. The task is an estimation of electric and magnetic fields amplitudes in an observation point situated near to the obstacle surface (up to distances, which have the same order as the obstacle surface). The following simplifications and approximations are introduced for the model development:

1) The environment is vacuum (relative permittivity and relative permeability are equal to 1, wave impedance $Z_0 = 120\pi$ Ohm, speed of light $c = 3 \cdot 10^8$ m/s).

2) The resistance of obstacle surface is zero.

3) Fraunhofer diffraction is not considered because the distances from the observation point to obstacle surface are comparable with the dimensions of obstacle and wavelength.

4) It is supposed that there are not through holes in obstacle. In the case of its presence, the consideration of diffraction by apertures is carried out additionally [14]. The obtained result for apertures (diffraction field strengths) is added by absolute value to the fields that result as diffraction by hull. This approach corresponds to the worst case behavior of the developed model.

Let us define a Local Coordinate System (LCS) with the origin in the observation point (see Fig. 1). The axis *Oy* is chosen in opposite direction to the Pointing vector of the

DOI: 10.1109/EMCEUROPE48519.2020.9245639

incident wave; axis *Oz* is chosen along the direction of incident wave polarization; axis *Ox* is directed perpendicular to *Oz* and *Oy* (right-hand system is considered).

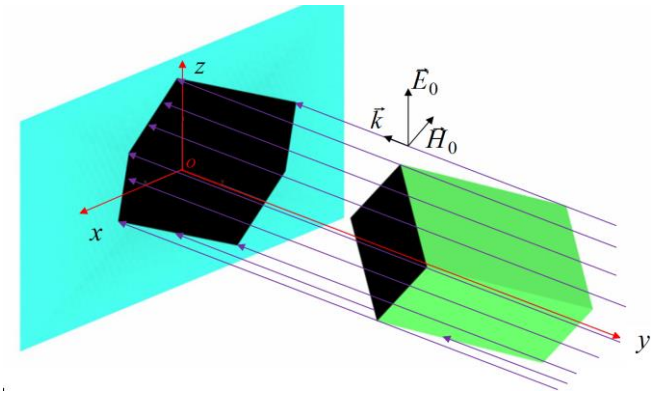

Fig. 1. Physical model of plane-wave diffraction by the surface of arbitrary shape, and LCS definition for the model development

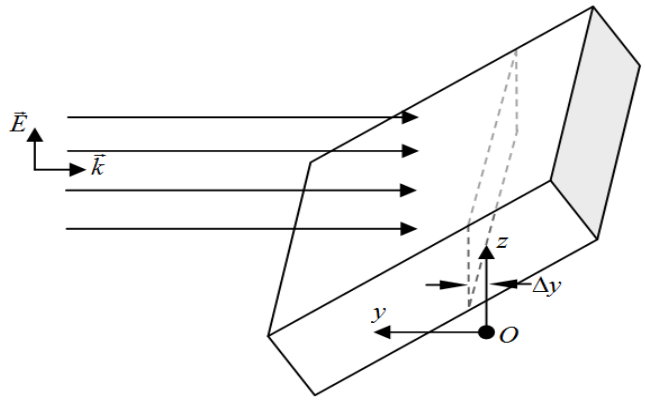

Fig. 2. Transformation of an obstacle geometry in case when the obstacle points have *y* coordinates of both signs in LCS

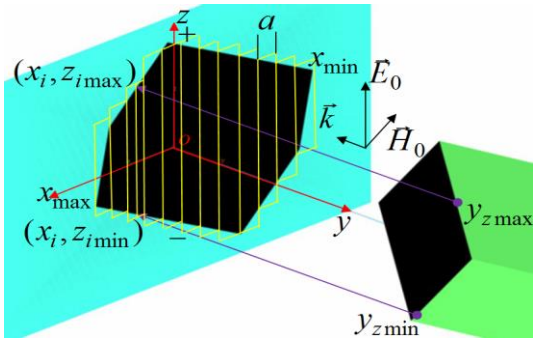

Fig. 3. Discretization of SZ in low-frequency range. The set of stripes is considered as dipoles

Coordinates of all points of the obstacle geometry are defined in LCS. The following cases are considered.

1) If coordinates $y_m > 0$ (m is a number of point) for all points of the obstacle geometry, then the obstacle is placed behind the observation point and conditions of Line of Side (LOS) are satisfied.

2) If coordinates $y_m < 0$ for all points of the obstacle geometry, then the obstacle is placed in front of the observation point (LOS conditions are critical for this case).

3) If coordinates of obstacle's points y_m have positive as well as negative values and LOS conditions are not satisfied, then all of points with coordinates $y_m \le \Delta y$ (where Δy is a small distance, see Fig. 2) are removed from consideration for analysis based on the Fresnel approach. This procedure provides the increasing of the calculated values of diffraction fields in observation point that corresponds to the worst case behavior of model.

The incident plane electromagnetic wave induced a distribution of electric charges and currents on the conductive surface of the obstacle. For the obstacles of arbitrary shapes, these distributions cannot be represented in analytical form, so, the diffraction fields cannot be obtained without the numerical integration.

In order to develop the computationally efficient semi-analytical model of diffraction, the discretization of geometry is realized not for obstacle, but for the shadow zone in projection on the corresponding plane *xOz* (the notation Shadow Zone (SZ) is introduced for this projection). Requirements to discretization are as follows: the dimensions of elementary parts after discretization must be as large as possible but must provide the sufficient accuracy in the representation of the SZ shape, and the distribution of electrical charges and currents at each elementary part can be defined in analytical form.

Low-frequency, resonance, and high-frequency ranges are introduced for the model development. Definition of the ranges corresponds to the physical processes, which determines the diffraction fields in the vicinity of an obstacle. In the low-frequency range, when the obstacle closes the small part of the first Fresnel zone for the observation point, the fields radiated by the electrical charges and currents induced by the incident wave make the main contribution to the distribution of diffraction field. For the high-frequency range, the distribution of diffraction fields is determined by the coherent secondary sources that belong to open area of the wave front in accordance with Huygens-Fresnel principle. Both effects make the contributions of the same order to formation of diffraction fields in resonance frequency range.

III. Model for Calculation of Diffraction Field Amplitudes in Low-Frequency Range

For the development of the model in low-frequency range, the SZ is divided to stripes of width *a*, which are parallel to the direction of the incident plane wave polarization. The SZ shape determines the value of parameter *a*, and the less parameter value the more accurate result of calculation will be obtained. The stripes are considered as a set of dipoles polarized by the incident wave along *Oz* axis, see Fig. 3. The following formula determines the resonance frequency of the dipole with the geometrical length L_g:

$$f_c = c/(2L_g). \qquad (1)$$

The low-frequency range is introduced in dependence on the length of each dipole and its upper boundary corresponds to $0.1f_c$.

The coordinates x_i of the central lines of strips parallel to *Oz* axis $[x_i - 0.5a, x_i + 0.5a)$ are introduced. The strip number is i, $i = 1 \ldots N$, $N = (x_{\max} - x_{\min}) / a$, $x_{\max}$, $x_{\min}$ are maximum and minimum coordinates of SZ in direction of *Ox* axis. The

geometrical lengths of dipoles corresponding to the strips are $L_{ig} = z_{i\max} - z_{i\min}$, where $z_{i\max}$, $z_{i\min}$ are maximum and minimum coordinates of i-th central line. Coordinate y_i of dipole center is chosen based on worst case requirements: $y_i = \min(y_{z\max}, y_{z\min})$, where $y_{z\max}$ is coordinate of the obstacle point, which corresponds to the point $(x_i, z_{i\max})$ on SZ and $y_{z\min}$ to the point $(x_i, z_{i\min})$. Finally, coordinates of i-th dipole center are: $(x_{c\,i}, y_{c\,i}, z_{c\,i})$, $y_{c\,i} = \min(y_{z\min}, y_{z\max})_i$, $z_{c\,i} = 0.5\cdot(z_{i\min} + z_{i\max})$.

The simplified quasi-static distribution of inducted electric charge on dipole is defined by the assumption that the electric charges of all others dipoles do not influence to the distribution of charge on dipole under consideration. So, the parameters of incident wave determine the distribution of electric charge only. Point charges of opposite signs are induced on the ends of dipoles with coordinates $z_{i\max}$ and $z_{i\min}$. The values of the charges are determined from the condition that the total electric field strength (the vector sum of the E-field of incident wave E_0 and field generated by the charges on the dipole ends) in the center of the dipole is zero.

$$q_i = 0.5\pi\varepsilon_0 E_0 L_i^{\,2}\sin(2\pi\cdot f\cdot t). \tag{2}$$

Quantity L_i in formula (2) is the dipole length, which in the framework of developed model depends on frequency of incident wave. Suppose that the dipole length is equal to the geometrical length of dipole $L_{i\,g}$ when it is less than the half of wavelength of incident wave. In this case, the free charges in a conductive strip have time for redistribution along entire length in a time equal to half of the oscillation period. With the increasing of the frequency, the charges do not have time for redistribution along the entire length, but they are redistributed at the distance, which is equal to half of the wavelength. For accounting this effect, formula for the dipole length takes the form

$$L_i = \min(L_{i\,g},\, c/(2f)). \tag{3}$$

Projections on LCS axis of quasi-static field generated by i-th dipole are as follows:

$$\begin{aligned}
&E_{szi} = \frac{-q_i}{4\pi\varepsilon_0}\left(b_{1i}^{-2}\cos\alpha_{1i} + b_{2i}^{-2}\cos\alpha_{2i}\right)\cdot F_{s_i},\\
&E_{sr\,i} = \frac{-q_i}{4\pi\varepsilon_0}\left(b_{1i}^{-2}\sin\alpha_{1i} - b_{2i}^{-2}\sin\alpha_{2i}\right)\cdot F_{s_i},\\
&b_{1,2\,i}^2 = r_i^2 + L_{pi}^2 \mp 2r_i\, L_{pi}\cos(\theta_i),\\
&\alpha_{1,2\,i} = \arctan\left(r_i\sin(\theta_i)/(L_{pi} \mp r_i\,\cos\theta_i)\right),\\
&E_{sxi} = E_{sr\,i}\cos\varphi_i,\; E_{syi} = E_{sr\,i}\sin\varphi_i,\\
&H_{si} = I_i\left(\cos(\alpha_{1i}) + \cos(\alpha_{2i})\right)/(4\pi r_i\sin(\theta_i)),\\
&H_{sx\,i} = H_{s\,i}\sin(\varphi_i), H_{sy\,i} = -H_{s\,i}\cos(\varphi_i), H_{sz\,i} = 0,
\end{aligned} \tag{4}$$

where $r_i^{\,2} = x_i^{\,2} + y_i^{\,2} + z_i^{\,2}$, $\theta_i = arcctg\,(z_i/\sqrt{y_i^{\,2} + x_i^{\,2}})$, $\varphi_i = \arccos(x_i/\sqrt{x_i^{\,2} + y_i^{\,2}})$ are coordinates of center of i-th dipole in spherical coordinates with the origin in the observation point (spherical LCS), I_i is current of i-th dipole.

Physically, the electric charge is not concentrated in the points on the dipole ends. For accounting this fact, and to define the correct transition from the low-frequency range to the resonance range, the factor $P_{L\,i}$ is introduced

$$P_{Li} = f/(f + 0.1 f_{ic}), \tag{5}$$

where $f_{ic} = c/(2\,L_{i\,g})$ is the critical frequency of i-th dipole and the correction factor $F_{s\,i}$ and physical half-length of dipole $L_{p\,i}$ for the quasi-static solution (4) can be written in the form as it was established empirically

$$\begin{aligned}
&F_{si} = 1 - P_{Li}\exp(-(L_{i\,g})/(2r_i)),\\
&L_{pi} = (0.45 + 0.05\cdot P_{Li})\cdot L_i.
\end{aligned} \tag{6}$$

This factor decreases the quasi-static solution at large distances from the obstacle for the frequencies that are near to the upper boundary of low-frequency range.

For analysis the electric and magnetic components of dipole radiation, let us consider the electric current inducted in dipole by E-field vector of incident wave of frequency f. The current is defined by the time derivative from the electric charge (2) and the current and electric moment for dipole of number i are as follows

$$\begin{aligned}
&I_i = \pi\varepsilon_0 f\cdot E_0\cdot L_i^{\,2}\cos(2\pi\cdot f\cdot t),\\
&p_{e\,i} = jI_{0i}\cdot L_i = j\pi\varepsilon_0 f\cdot E_0\cdot L_i^{\,3}(2 + P_{L\,i}).
\end{aligned} \tag{7}$$

In accordance with equation (3), for wavelengths, which are more than geometrical length of dipole, dipole moment increases proportional to the frequency, and when the frequency is more than critical frequency, it decreases as a square of frequency. Factor $(2 + P_{L\,i})$ is introduced to take into account the increasing of directivity of dipole when the frequency tends to the critical frequency.

In framework of developed model, for calculation the radiation fields of dipole, the following modified formulas of the short dipole are used in spherical LCS:

$$\begin{aligned}
&E_{d\,ri} = 2K_i\cos\theta_i\left[(k\,r_i)^{-2} - j(k\,r_i)^{-3}\right]\cdot F_{d\,i},\\
&E_{d\theta i} = K_i\sin\theta_i\left[j(k\,r_i)^{-1} + (k\,r_i)^{-2} - j(k\,r_i)^{-3}\right]\cdot F_{d\,i},\\
&H_{d\,\varphi i} = \frac{K_i}{Z_0}\sin\theta_i\left[j(k\,r_i)^{-1} + (k\,r_i)^{-2}\right]\cdot F_{d\,i},\\
&K_i = \frac{p_{ei}}{4\pi}Z_0 k^2,\quad k = \frac{2\pi\cdot f}{c},\\
&F_{d\,i} = (1 + P_{Li})\exp(-(L_{i\,g})/(2r_i)),
\end{aligned} \tag{8}$$

where the correction factor $F_{d\,i}$ eliminates the contribution of solution (8) near the center of dipole, which has not a physical interpretation.

Projections of dipole fields (8) to axis x, y, z of LCS are

$$
\begin{aligned}
&(E_{dri})_z = E_{dri}\cos\theta_i,\ (E_{dri})_x = E_{dri}\sin\theta_i\cos\varphi_i,\\
&(E_{dri})_y = E_{dri}\sin\theta_i\sin\varphi_i,\\
&(E_{d\theta i})_z = E_{d\theta i}\sin\theta_i,\ (E_{d\theta i})_x = E_{d\theta i}\cos\theta_i\cos\varphi_i,\\
&(E_{d\theta i})_y = E_{d\theta i}\cos\theta_i\sin\varphi_i;\\
&(H_{d\varphi i})_x = H_{d\varphi i}\sin\varphi_i,\ (H_{d\varphi i})_y = H_{d\varphi i}\cos\varphi_i.
\end{aligned}
\tag{9}
$$

The sum by index i of pseudo-static and dipole radiation fields in projections to axis of LCS is performed taking into account the phases and directions defined by formulas (4) and (8). The summarized dipole field is averaged by the number of dipoles N.

$$
\begin{aligned}
&E_{sdz} = N^{-1}\sum_{i=1}^{N}(E_{szi} + (E_{dri})_z + (E_{d\theta i})_z),\\
&E_{sdx} = N^{-1}\sum_{i=1}^{N}(E_{sxi} + (E_{dri})_x + (E_{d\theta i})_x),\\
&E_{sdy} = N^{-1}\sum_{i=1}^{N}(E_{syi} + (E_{dri})_y + (E_{d\theta i})_y),\\
&H_{sdx} = N^{-1}\sum_{i}(H_{d\varphi i})_x,\ H_{sdy} = N^{-1}\sum_{i}((H_{d\varphi i})_y.
\end{aligned}
\tag{10}
$$

It is established empirically, that for resonance frequency range, which is determined for each dipole in the frequency range from $0.1f_{ic}$ to $4f_{ic}$, the following correction based on the dipole model is useful. The integer number $V_i = ceil(f / f_{ic})$ is introduced, where operation *ceil* returns value 1 for all arguments, which are less or equal to 1, value 2 for arguments which are more than 1 and less or equal to 2, etc. For $V_i = 2$, the field of two dipoles with the centers in the points $(x_i, y_{ci}, z_{ci} \pm 0.25L_{gi})$ are considered by use formulas (4), (8) – (10). For $V_i = 3$, the centers of three dipoles have coordinates (x_i, y_{ci}, z_{ci}) and $(x_i, y_{ci}, z_{ci} \pm (1/3)L_{gi})$, and for $V_i = 4$, the centers of the dipoles are $(x_i, y_{ci}, z_{ci} \pm (1/8)L_{gi})$ and $(x_i, y_{ci}, z_{ci} \pm (3/8)L_{gi})$. The currents in neighboring dipoles are opposite. For frequencies between f_{ic} and $2f_{ic}$, ($2f_{ic}$ and $3f_{ic}$, etc.), the values of projections of field strength is obtained by the use of connection function, which takes the form:

$$
E(f) = E(kf_c)(1 - F_{tr}(f)) + E((k+1)f_c)F_{tr}(f), \tag{11}
$$

where $E(kf_c)$ are defined for the set of frequencies $k = 1\ldots4$ by formulas (4) and (8); $F_{tr}(f)$ is the weighting function:

$$
F_{tr}(f) = 3(\chi(f))^2 - 2(\chi(f))^3,\ \chi(f) = (f - kf_c)/f_c. \tag{12}
$$

IV. Model for Calculation of Diffraction Fields by Using of Fresnel Approach

The approach for development of the model in resonance and high-frequency ranges is based on the consideration of Fresnel zones. In the plane of SZ (xOz), the polar LCS is defined as follows: the angle φ is counted from Ox axis and the distance l is measured from the observation point O to the projection of the point belonging to obstacle onto xOz plane.

The discretization of SZ is performed as follows. The initial angle φ_0 and interval of angles $\Delta\varphi = 2\pi / M$ are chosen. Half-planes passing through the Oy axis at angles φ_0 and $\varphi_0 + m\cdot\Delta\varphi$, $m = 1\ldots M$ are built. The intersection points of the planes with the boundary of SZ (contour) have coordinates in LCS: $\varphi_m = arctg(z_m / x_m)$, $l_m = \sqrt{x_m^2 + z_m^2}$.

Each sector between planes of numbers m and $m+1$ obtained by the procedure described above is considered as the sector of Fresnel zone. The total diffraction field E_{FD} is calculated as the sum by index m of contributions corresponding to each sector.

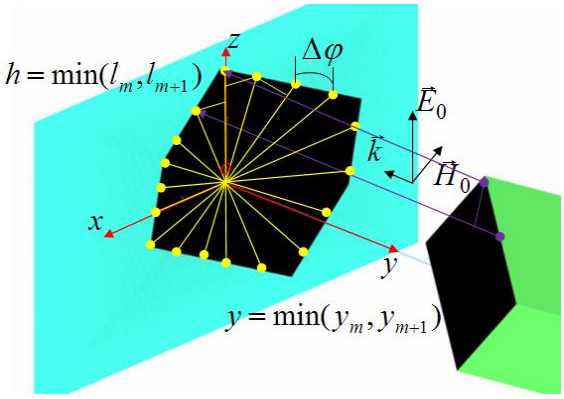

Fig. 4. Discretization of SZ to sectors

If one of the plane defining the sector has not intersection points with SZ contour, then the sector is an opened sector and its contribution to the total diffraction field is equal to $E_m = E_0 / M$.

When both of the planes bounding the sector have intersection points with the SZ contour, the following procedures are performed.

1) On each half-plane, choose intersection points, which are nearest to the observation point at distances l_m and l_{m+1} respectively. Define a center mass of triangle, which is built on three points: observation point, and the nearest points of intersections of half-planes and contour.

2) If the center mass of the triangle belongs to SZ, then the height of an equivalent obstacle corresponding to m-th sector is $h_{m1} = \min(l_m, l_{m+1})$. The distance from observation point to the equivalent obstacle is $y_{m1} = \min(y_m, y_{m+1})$, see Fig. 4.

3) Define the critical frequency of the sector f_{mc} and correction factor Q_{Fm} by formulas

$$
f_{mc} = c/(2h_m),\ \ Q_{Fm} = f/(f + f_{mc}). \tag{13}
$$

The correction factor Q_{Fm} defines the contribution of the sector to the field strength calculated based on Fresnel approach. The inequalities $h_{m1} >> \lambda$, $y_{m1} >> \lambda$ determine the restriction on the Fresnel principle using. If the inequality is not satisfied (that is true for frequencies less than f_{mc}), then the sector m is considered as opened sector and the contribution tends to the value $E_m = E_0 / M$.

4) Calculate the number of Fresnel zones, which corresponds to the equivalent obstacle of the height h_m placed on the distance y_m from the observation point by formula (14).

$$
n_m = 2y_m / \lambda\left(\sqrt{1 + (h_m / y_m)^2} - 1\right). \tag{14}
$$

5) The contribution of the sector is calculated by formula

$$E_m = T_m^{Q_{Fm}} \cdot E_0 / M . \quad (15)$$

where T_m is the factor, which takes into account the dependence of contribution of secondary coherent sources, which are not closed by obstacle, on the distance $d_m = \sqrt{h_m^2 + y_m^2}$ from observation point to Fresnel zone, and angle between normal to Fresnel zone and direction to observation point. This factor is calculated by the formula

$$T_m = \frac{y_m^2}{(y_m + 0.5 \cdot n_m \cdot \lambda)^2} \exp(j\pi n_m) \quad (16)$$

6) If the center mass of triangle considered in item 1) does not belong to SZ, then there must be at least two points of intersection between bounding half-planes and contour. Denote coordinates of these points as y_{2m}, y_{2m+1} and distances from LCS center to them as l_{2m} and l_{2m+1}. The following contribution corresponds to the sector in this case:

$$\begin{aligned} E_m &= (R_m + S_m)^{Q2_{Fm}} \cdot E_0 / M, \\ R_m &= 1 - T_m, \end{aligned} \quad (17)$$

where R_m corresponds to the contribution of Fresnel zones, which are opened in limits of the area of the nearest triangle, S_m corresponds to the Fresnel zones, which are opened in the area of the sector placed out of the distance $h_{m2} = \min(l_{2m}, l_{2m+1})$, (contribution $Q2_{Fm}$ is defined by (13) by substitution h_{m2} in it). Calculation of S_m is performed by (14)-(16) for $y_{m2} = \min(y_{2m}, y_{2m+1})$. If there are more than 2 opened areas within the sector, the corresponding summands are added in sum (17).

Procedures described in items 1)-4) are repeated for all of SZ sectors and the sum by sectors from 1 to M defines the contribution of Fresnel diffraction: $E_F = \sum E_m$, $H_F = \sum H_m$.

Note, that for high frequencies, analytical expression obtained by integration of equation presented in [15]

$$E_{FA} = M^{-1} \sum (j \exp(jkr_m) y_m / r_m), \; r_m = \sqrt{y_m^2 + h_m^2} \quad (18)$$

provides the more accurate value of field magnitude than the method proposed above, and the maximum value from E_F and E_{FA} will be used for the worst case model.

V. Combined Solution and Worst Case Model of Plane-Wave Difraction by Conductive Obstacle

A combined wideband solution is constructed as a sum of projections of E-field and H-field strengths obtained for all of frequency ranges. Note that in accordance with the problem statement, the incident wave is polarized along Oz axis of LCS (H-field is directed along Ox axis). So, the diffraction fields in the shaded zone are calculated as follows:

$$\begin{aligned} &E_{Dz} = E_{sd\,z} + \max(E_F, E_{FA}), E_{Dx} = E_{sd\,x}, E_{Dy} = E_{sdy}; \\ &H_{Dx} = H_{sd\,x} + \max(H_F, H_{FA}), H_{Dy} = H_{sd\,y}, H_{Dz} = 0; \\ &E_D = \sqrt{E_{Dx}^2 + E_{Dy}^2 + E_{Dz}^2}, \; H_D = \sqrt{H_{Dx}^2 + H_{Dy}^2 + H_{Dz}^2}, \end{aligned} \quad (19)$$

where the low-frequency solution based on the dipole approximation is obtained by the use of formula (10).

Let us discuss the physical meaning of the obtained combined solution. In the low-frequency range, the dipole solution defines the distribution of resulting field because only a little part of the first Fresnel zone is closed for the observation point. In this case, $E_F = E_0$. With the increasing of the frequency, the contribution of the dipole solution decreases due to the decrease. At the same time, the contribution of the Fresnel approach increases. As a result, in the resonance- and high-frequency ranges, maximums and minimums of the field distribution arise in the framework of the combined wideband solution (19).

To develop a worst case model of spatial field distribution based on solution (19) it is necessary to define its worst case envelope, which is defined in framework of the following algorithm.

1) For the fixed frequency, calculate the field strength magnitude in the points situated on the plane, which is perpendicular to Oy axis and has coordinate y_j. The set of planes with distances Δy between them is considered.

2) Define the minimum value of field magnitude at the ends of interval of coordinates (x_i, $x_i + \Delta x$) (y_j, z_k are fixed) and variation of the field magnitude due to the variation of coordinates in the plane:

$$\begin{aligned} E_{Dix} &= \min\{E_D(x_i), \; E_D(x_i + \Delta x)\}, \\ \Delta E_{Dix} &= E_D(x_i + \Delta x) - E_D(x_i). \end{aligned} \quad (20)$$

3) Obtain the coordinates x_i of points, where the variation ΔE_{Dix} changes the sign from positive to negative. These points are the points of local maximums.

4) For intervals of the monotonous changing of field, add the value ΔE_{Dix} to the minimum value E_{Dix} in the corresponding point that belongs to considered interval.

5) Connect the points obtained in items 3) and 4) on the graph of dependence of field magnitude on x coordinate. This new graph consisting of segments connects the points of graph of solution (19) is the worst case model of spatial field distribution in the plane y_j for the line z_k.

6) Repeat steps described in items 2) – 5) for all lines z_k in the plane y_j.

7) Fix the coordinate x_i and perform steps 2) – 5) for the case of variation of z_k.

8) Perform item 6) for all lines x_i in the plane y_j.

9) Consolidation of results, obtained in items 5) and 7) is the worst case model of field distribution in the plane y_j.

10) Perform items 2) – 7) for all of planes y_j to obtain the worst case model of field distribution in the region under consideration.

To develop a worst case model of the amplitude-frequency characteristic (AFC) of a field in the fixed spatial point, the field magnitude is calculated by formula (19) for the set of frequencies. After that the procedure of worst case envelope definition (see items 2) – 5) of previous algorithm) is applied on the frequency grid.

VI. Validation of Developed Model

The validation is performed by comparison of the results obtained in framework of the developed model based on combined solution (19) with results of numerical simulation using MOM and FDTD methods. The following example is considered. A parallelepiped with dimensions 3×4×7 m is irradiated by a plane wave with amplitude 1 V/m (as shown in Fig. 1), and the field distribution along a straight line located behind the parallelepiped is computed (Fig. 5).

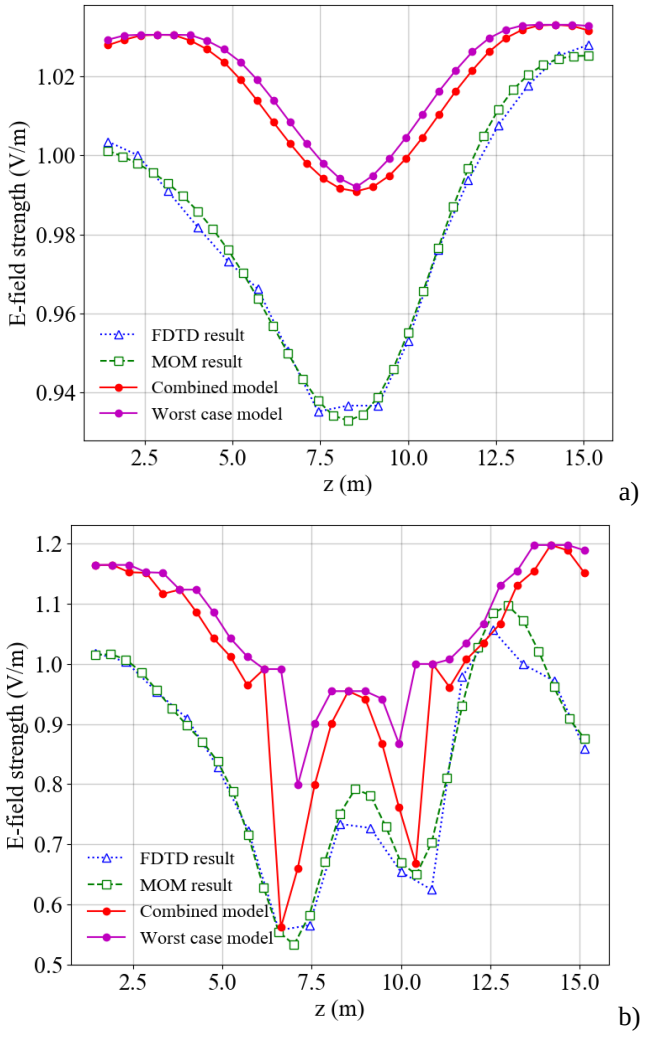

Fig. 5. Dependence of the electric field intensity on coordinate z of observation point: a) f = 1 MHz; b) f = 100 MHz. Note: coordinates (x, y, z) of the parallelepiped center are (-13.6 m, 0 m, 8.5 m), and the coordinates of the observation point are (-11.8 m, -7.2 m, z).

The duration Δt of field intensity calculation by the developed technique is less than 300 ms for each observation point; it does not depend on both the frequency and the distance from the parallelepiped to an observation point. The durations of the calculations performed by MOM and FDTD methods increase with increasing of the frequency, e.g., at the frequency of 100 MHz they are as follows: Δt_{MOM} = 5 s for each observation point and Δt_{FDTD} = 95 s for all points.

VII. Conclusion

The developed model makes it possible to perform a fast estimation of the amplitude of diffraction field near the system hull made of conductive materials in a wide range of frequencies. The results of this estimation can be used for analysis of the impact of a complex EME (including a wideband EM pulse disturbance) on the system through the on-board antennas and through the apertures in the hull.

The hints for future developments of the model are as follows: to consider the diffraction fields in the Fraunhofer zone, to analyze the reflected fields in LOS zone, and to account for the antenna pattern when calculating the impact of diffraction fields on antennas.

References

[1] Siegel M.D. “Aircraft antenna-coupled interference analysis”, Proc. Nat. Aerospace Electron. Conf., Dayton,Ohio, 1969. pp. 535-540.

[2] Bogdanor J.L., Pearlman R.A., Siegel M.D. Intrasystem Electromagnetic Compatibility Analysis Program: Volume I – User’s Manual Engineering Section, Mc.Donnel Douglas Aircraft Corp., F30602-72-C-0277, Rome Air Development Center, Griffiss AFB NY, Dec. 1974.

[3] Baldwin T.E., Robinson R.C., Duff W.C., Schumann H.K., Foster J.J., Bartley M.K. Intrasystem analysis program (IAP) model improvement: Final Technical Report, Atlantic Research Corp., F30602-79-C-0169, Rome Air Development Center, Griffiss AFB NY, February, 1982.

[4] V. Mordachev et al., “EMC diagnostics of complex radio systems by the use of analytical and numerical worst-case models for spurious influences between antennas,” 2016 International Symposium on Electromagnetic Compatibility – EMC EUROPE, Wroclaw, 2016, pp. 608–613.

[5] EMC-Analyzer. Mathematical models and algorithms of electromagnetic compatibility analysis and prediction software complex. Minsk, 2020.

[6] Tsyanenka D.A., Sinkevich E.V., Matsveyeu A.A. “Computationally-Effective Worst-Case Model of Coupling between On-Board Antennas That Takes into Account Diffraction by Conducting Hull,” 2016 International Symposium on Electromagnetic Compatibility – EMC EUROPE, Wroclaw, 2016, pp. 602-607

[7] Christopoulos Cr. “Modeling and simulation for EMC, Part 1,” IEEE Electromagnetic Compability Magazine, Vol. 4, 2015, p. 47-55.

[8] Saez de Abana F., Gutierrez O., Perez J., Catedra M.F.. “Computer tool for the analysis of antennas on board complex bodies modelled by flat or/and curve facets,” Antennas and Propagation Society International Symposium, IEEE, 1998, Vol. 2, p. 1082-1084.

[9] Booton R. Computational methods for electromagnetics and microwaves, John Willey & Sons, New York, 1992.

[10] Pathak P.H. High-frequency techniques for antenna analysis/ Proc. of the IEEE, 80, January, 1992, p. 44-65.

[11] C. Fang, Q. Zhang, Q. Huang and Y. XuanYuan, "The predicted technique of EMI for ship radars based on the GTD revision," 2011 China-Japan Joint Microwave Conference, Hangzhou, 2011, pp. 1-3.

[12] Davidson S.A., Thiele G.A. “A hybrid method of moments – GTD technique for computing electromagnetic coupling between two monopole antennas on a large cylindrical surface,” IEEE Transactions of electromagnetic compability, Vol. EMC-26, No 2, 1984, p. 90-97.

[13] Srikanth S., Pathak P.H., Chuang G.W. “Hybrid UTD-MM analysis of the scattering by perfecly conducting semicircular cylinder,” IEEE Transactions on Ant. and Propagation, Vol. 34, 1986, p. 1250-1257.

[14] Tsionenko D., et al. “Computationally-Effective Ultra-Wideband Worst-Case Model of Electromagnetic Wave Diffraction by Aperture in Conducting Screen” 2014 Int. Symp. on EMC -- EMC Europe 2014”, Gothenburg, Sweden, 2014, pp.1287-1292.

[15] Ustinov A. V. “The fast way for calculation of first class rayleigh-sommerfeld integral” Computer optics, Vol. 33, No. 4, pp. 412-419